Desalination and Water Treatment
www.deswater.com

doi: 10.5004/dwt.2019.23753

147 (2019) 273–283
April

Modeling of adsorption isotherms of (5,5′-disodium indigo sulfonate) from aqueous solution onto activated carbon: equilibrium, thermodynamic studies, and error analysis

Zahia Harrache[a], Moussa Abbas[a,*], Tounsia Aksil[a], Mohamed Trari[b]

[a]*Laboratory of Soft Technologies and Biodiversity, Faculty of Sciences, University M'hamed Bougara Boumerdes, Boumerdes 35000, Algeria, Tel. +213 552408419; Fax: +213 21 24 80 08; emails: moussa_abbas@gmail.com (M. Abbas), ZAHIA_HARRACHE@yahoo.fr (Z. Harrache), tounsiaiap@gmail.com (T. Aksil)*
[b]*Laboratory of Storage and Valorization of Renewable Energies, Faculty of Chemistry (USTHB), BP 32-16111 Algiers Algeria, email: solarchemistry@gmail.com*

Received 8 July 2018; Accepted 5 January 2019

ABSTRACT

The activated carbon (AC) and its ability to remove dyes (5,5′-disodium indigo sulfonate, Indigotine I, blue CI *n*°1, Indigo carmine (IC) used in textile and biology from aqueous solution are investigated. The kinetic and equilibrium parameters of the adsorptative adsorption for IC removed by AC were studied by UV-visible absorption spectroscopy. The present work deals with the adsorption of IC dyes on AC, and the effects of parameters affecting the adsorption capacity were determined to find the optimal conditions for obtaining the maximum amount of adsorption. The physicochemical characteristics of the AC were characterized by BET method and point of zero charge. The adsorption mechanism of IC onto AC was studied; the adsorption kinetics was found to follow a pseudo-second-order kinetic model. The equilibrium adsorption data for IC on AC were analyzed by several models. The smaller root mean square error values for the Langmuir and Dubinin-Radushkevich models indicate the best fitting; the monolayer adsorption capacity of IC was found to be 249 mg/g at 25°C and 298.34 mg/g at 40°C at pH 2. The adsorption isotherms at different temperatures have been used to obtain thermodynamic parameters: the free energy ($\Delta G° = -0.71$ to -1.01 kJ/mol), enthalpy ($\Delta H° = 28.11$ kJ/mol), and entropy ($\Delta S° = 0.093$ kJ/mol K) of adsorption with activation energy E_a of 51.06 kJ/mol. The negative $\Delta G°$ and positive $\Delta H°$ values indicate that the overall adsorption is spontaneous and endothermic. This study in tiny batch gave rise to encouraging results and we wish to achieve the adsorption tests in column mode under the conditions applicable to the treatment of industrial effluents, and the present investigation showed that AC is a potential useful adsorbent for the dyes.

Keywords: Indigotine; Removal; Kinetics; Equilibrium; Thermodynamics; Modeling; Isotherm; Mechanism

1. Introduction

Dyes are commonly used in many industries, like textile, food, paper, plastic, cosmetics, and coloring industries. These industries commonly use synthetic dyes as colorants. Discharge of dyes contained in wastewaters contaminates both the surface water and ground water. However, 7 × 10 t of dye stuff are produced annually. The dyes even at very low concentrations affect the aquatic life and human health by polluting the environment. The toxicity and carcinogenicity have lead to exploration of possible detoxicants. Dyes can cause allergies, dermatitis, skin irritation, cancer, mutation, etc. In general, dyes are poorly biodegradable, and some of them produce aromatic amines which are highly

* Corresponding author.

carcinogenic. Many investigators have studied the feasibility of inexpensive alternative materials like pearl millet husk, date pits, sawdust, buffing dust of leather industries, coir pith, crude oil, residue, tropical grass, olive stone, apricot stone, almond shell, pine bark, wool waste, coconut shell, etc. Indigo carmine (IC) is a water-soluble derivative of the famous indigo disulfonate which has great applications in the textile industry [1]. It has also been used as additive in pharmaceutical tablets and as coloring agent in confectionery, food, beverages, and cosmetics. It also serves as a diagnostic aid, as oxidation-reduction indicator in analytical tests, and as microstain in biology [2]. IC is an acid dye [3,4] and is therefore used to dye protein fibers, wool, and silk [5], including the use of alum as a bite in the latter case [6]. Limited studies are available on the adsorption of IC on the silk and wool, in particular with regard to dyeing and the removal of effluents from textile treatments [7]. The textile industry around the world and the growing demand for ceramic paper, printing, and plastics use a wide variety of dyes as raw materials [8]. Dyes are also used in medicine, biological strains, and plastic staining [9]. Waste from these industries, in one way or another, ends up in water, thus polluting the environment. Unlike other pollutants, coloring pollutants, especially those with benzene rings, even at low concentrations, are visible, reducing the penetration of light in water, which has a negative effect on the photosynthesis of aquatic plants [10]. Similarly, the human activities have caused great damages to the quality of our lifeline, namely, water [11]. IC is also used as additive in pharmaceutical tablets and capsules and for medical diagnostic purposes. Indeed, the dye injection for cystoscopy is a safe technique for detecting compromises in the urinary tract implant [12]. It is considered a highly toxic class of industrial dye, and its touch can cause skin and eye irritation as well as permanent damage to the cornea and conjunctiva. Consumption of the dye can also be fatal because it is importantly carcinogenic and can lead to reproduction, development, neurotoxicity and acute toxicity. Wastewater containing IC dye is rich in color and organic content and a large amount of suspended solids whose pH, temperature, and chemical oxygen demand vary considerably [13]. According to United Nations Educational, Scientific and Cultural Organization standards and the World Health Organization, the IC at a concentration above 0.1 mg/L [14] is not acceptable in water. This dye is a nuisance not only for aquatic life but also for the human. The treatment of this waste before disposal is therefore essential. Some treatments for the removal of heavy metals and aqueous solutions have been reported: one can cite the ion exchange, electrochemical reduction, evaporation, solvent extraction, reverse osmosis, chemical precipitation, membrane filtration, adsorption, etc. Depending on the nature of aqueous effluents, flow rates, and metal concentrations, the industrial application of these processes is restricted by the operating costs or inefficiency of the adsorption technique. These methods differ in their effectiveness in removing the IC dye from water; they have certain disadvantages, including high investment and operating costs and the need for appropriate treatment and disposal of residual dye sludge [15].

This study was carried out with the aim to optimize the initial dye concentration, pH, particle size, contact time, adsorbent dose, agitation speed, and temperature for the IC uptake. In addition, the equilibrium adsorption data were fitted to various equations for the determination of constants related to the adsorption phenomena. Equilibrium and kinetic analysis were conducted to determine the factors controlling the adsorption rate, the optimization of physical parameters in the dye recovery, and to find out the possibility of using this activated carbon (AC) for the dye removal. This study has given encouraging results and we wish to carry out column adsorption tests under the conditions applicable to the treatment of industrial effluents, and to test the homogeneous photodegradation of IC by TiO_2, ZnO, and SnO_2 semiconductors is the future objective of this work.

2. Experimental

2.1. Determination of zero point charge pH$_{(zpc)}$

The zero point charge (pH$_{(zpc)}$) of AC, i.e. the pH for which the surface charge is null, is determined using a procedure similar to that described elsewhere [16]. Two hundred milliliters of $NaNO_3$ solutions (0.01 M) are placed in closed conical flasks; the pH of each solution is adjusted between 2 and 14 by addition of HCl or NaOH solution. Then 0.1 g of AC is added, and the final pH is measured after 24 h under agitation at room temperature. pH$_{(zpc)}$ is the point where the final pH versus initial pH crosses the line of final pH = initial pH.

2.2. Batch mode adsorption studies

The effects of the experimental parameters such as the initial IC concentration, pH, adsorbent dose, and temperature on the IC removal are studied in batch mode for a specific period of contact time. The stock solution is prepared by dissolving the accurate amount of IC (99%, Merck) in distilled water; the other solutions are prepared by dilution. pH is adjusted with HCl or NaOH. The characteristics of IC are represented in Table 1. The IC content in the supernatant is analyzed on a Perkin Elmer UV-Visible spectrophotometer model 550S (λ_{max} = 610 nm). The amount of IC adsorbed on AC q_t (mg/g) is calculated from the following equation:

$$q_t = \frac{(C_0 - C_t)}{m} \times V \tag{1}$$

where C_0 is the initial IC concentration, C_t the IC concentrations (mg/L) at time (t), V the volume of solution (L), and m the mass of the AC (g). Due to the inherent bias resulting from the linearization of the isotherm and kinetic models, the nonlinear regression (root mean square error, RMSE) evaluated in Eq. (2) is used as criterion for the quality of fitting [17]:

$$\text{RMSE} = \sqrt{\frac{1}{N-2} \times \sum_{1}^{N} \left(q_{e,\exp} - q_{e,\text{cal}}\right)^2} \tag{2}$$

where $q_{e(\exp)}$ (mg/g) is the experimental value of uptake, $q_{e(\text{cal})}$ the calculated value using a model (mg/g), and N the

Table 1
General characteristics of Indigo carmine (IC) dye

Chemical name	IC, Indigotine
IUPAC name	5,5′-disodium indigo sulfonate
Color index	Acid blue 74, N° 73015
Chemical formula	$C_{16}H_8N_2Na_2O_8S_2$
Molar mass (g/mol)	466.360 ± 0.026
λ_{max} (nm)	610
Solubility in water	10 g/L at 25°C
Chemical structure	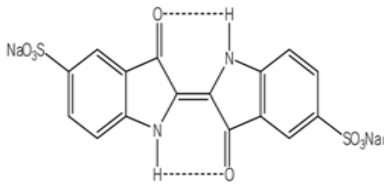

number of observations in the experiment (the number of data points). The sum of error squares (SSE) is widely used to test the validity of each model [18]:

$$\mathrm{SSE} = \frac{1}{N} \times \sum_{1}^{N} \left(q_{e,\exp} - q_{e,\mathrm{cal}} \right)^2 \tag{3}$$

The chi-square statistic is given by Eq. (4):

$$\chi^2 = \sum_{1}^{N} \frac{\left(q_{e,\exp} - q_{e,\mathrm{cal}} \right)^2}{q_{e,\mathrm{cal}}} \tag{4}$$

If the data from the model ar[illegible] nila[illegible] to th[illegible] erimental ones, χ^2 is small. Conversely, if the[illegible] ifferent, [illegible]ecomes large. The small the RMSE and χ^2 [illegible] the better [illegible]urve fitting.

3. Results and discussio[illegible]

3.1. Characterization of t[illegible]AC

Th[illegible] surfac[illegible]d pore [illegible]cture of the ACs we[illegible]ulat[illegible]y the [illegible]equation [illegible]g the ASAP 2010 [illegible]omeritics [illegible]ipment. [illegible] surface area, micro[illegible]ore area, an[illegible]icropore volu[illegible] were determined by the [illegible]-plot metho[illegible] 1). The total pore volume was evaluated [illegible]m the [illegible] a high relative pressure near [illegible] (Fig. 2). The pore size distribution was deter[illegible]min[illegible]sing the density functional theory model (Fig. 3). The [illegible]ore volume was calculated by subtracting the micropo[illegible]lume from the total volume. The parameters calcula[illegible]rom the isotherm diagrams and *t*-plot are gathered in Table 2.

3.2. Optimization study of operating conditions

The pH plays an important role in the adsorption process and particularly on the uptake capacity. It is observed that the percentage of IC removal decreases consistently with increasing pH (Fig. 4). The pH effect on IC adsorption by AC can be explained on the basis of $pH_{(zpc)} = 5.23$ (Fig. 5). The AC surface charge is negative above $pH_{(zpc)}$. So, as the pH of the solution increases, the number of positively charged sites decreases and favors the IC adsorption by electrostatic attractions.

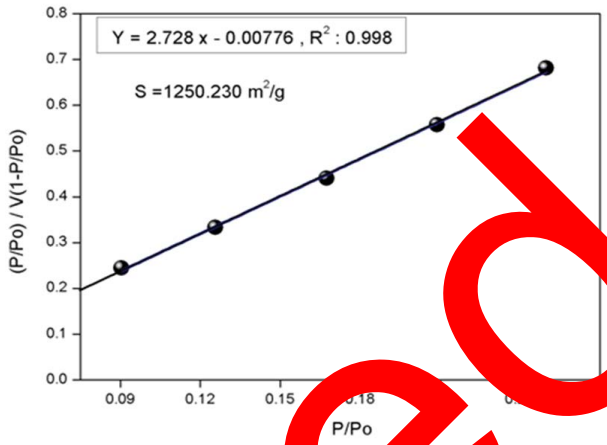

Fig. 1. Determi[illegible]tion of the [illegible]ecifi[illegible]rface a[illegible] by the *t*-plot method.

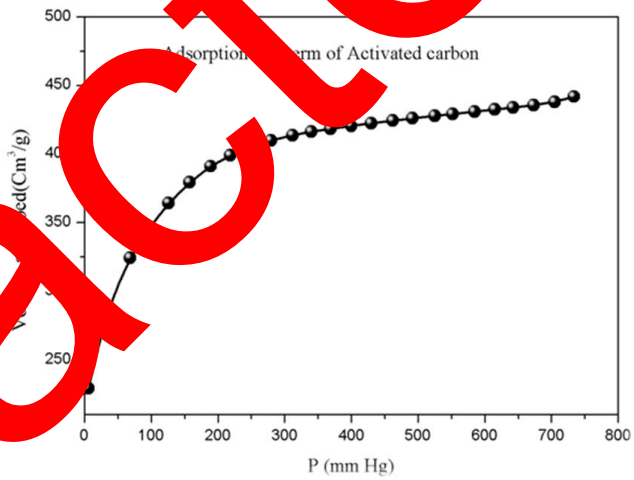

Fig. 2. Adsorption isotherm of activated carbon.

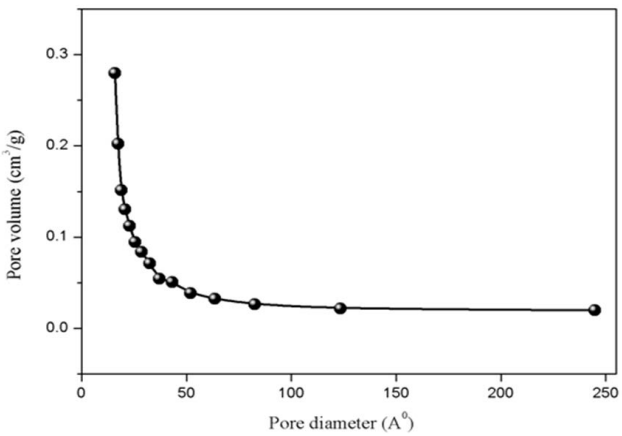

Fig. 3. Pore volume distribution.

The effect of the stirring speed in the range 100–1250 rpm on the adsorption capacity onto AC is also investigated. The optimal adsorption capacity is obtained for a speed of 400 rpm which gives the best homogeneity of the mixture suspension. Therefore, a speed of 400 rpm is selected for further experiments.

Table 2
Physicochemical characteristics of activated carbon

Specific surface area (m^2/g)	Porous volume (cm^3/g)
S_{BET}: 1,250.230	V_T: 0.6834
S_{ext}: 527.372	V_{mes}: 0.6684
S_{mic}: 753.332	V_{mic}: 0.0150
Pore diameter per density functional theory (nm)	1.581
Particle size (mm)	1.25 < Ø < 2.5
Humidity (%)	0.737
Moisture content (%)	0.743
Apparent density (g/cm^3)	0.506
Reel density (g/cm^3)	1.249
Total pore volume (cm^3/g)	1.176
Total porosity	0.595

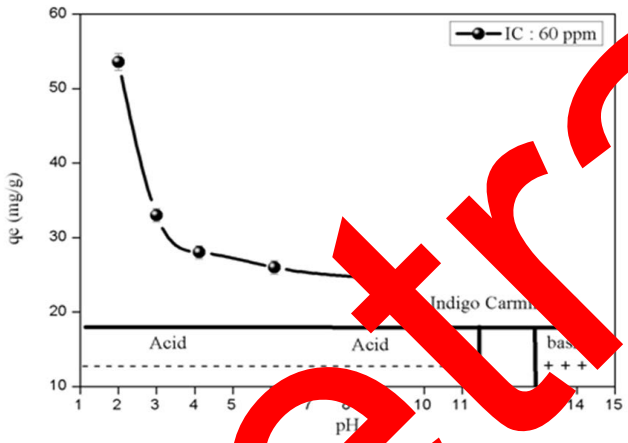

Fig. 4. Effect of pH on I[illegible]dsor[illegible] by AC

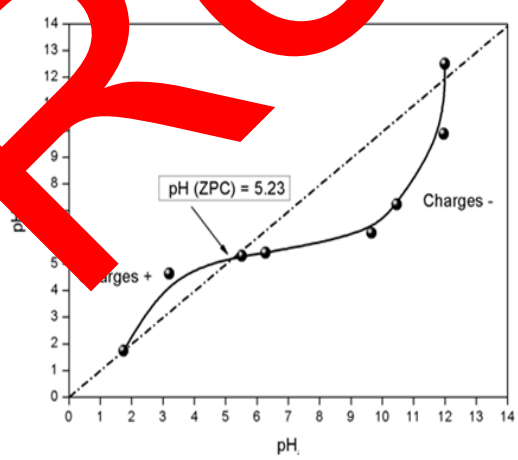

Fig. 5. Determination of pH of zero point charge $pH_{(ZPC)}$ of AC.

The effect of adsorbent dose on the IC removal shows that this parameter influences the adsorption. It can be seen from the curve $q_t = f$ (adsorbent dose) that the adsorption capacity is inversely proportional to the a[illegible]rbent dose. Significant variations in the uptake capacity [illegible] elimination efficiency are observed at different adsor[illegible] doses (1–10 g/L), indicating that the best perform[illegible]e is [illegible]ned for an adsorbent dose of 1 g/L; this optim[illegible]alue is reta[illegible]d for further experiments and isotherm plo[illegible]

The adsorption capacity of IC increas[illegible]over time an[illegible] reaches a maximum after 45 min of contac[illegible]e and the[illegible] after tends toward a constant [illegible]ating [illegible]e IC ions are further remove[illegible]rom th[illegible]lution. [illegible] equilibrium time averages 45 [illegible]in, bu[illegible]r pr[illegible]tical reasons, the adsorptio[illegible] is run up [illegible]90 [illegible]. By ra[illegible]ng the initial IC concentrati[illegible]C [illegible]rom [illegible] mg/L, t[illegible]amount of IC adsorbed increas[illegible]om 2.40 [illegible]35 mg/[illegible]g. 6). The optimum values ob[illegible]om the o[illegible]n of the analytical parameters are repres[illegible]d in Table 3.

3.3. A[illegible]rption isotherms

T[illegible] shape of the [illegible]otherms is the first experimental tool t[illegible]agnose the [illegible]ture of a specific adsorption. The

T[illegible]
[illegible]ptim[illegible] value parameters for the isotherm plots

Para[illegible]ter	Optimum value
p[illegible]	2
[illegible]article size (mm)	1.0 < Ø < 2.0
Contact time (min)	45
Stirring speed (trs/min)	400
Adsorbent dose (g/L)	1
$pH_{(ZPC)}$	5.23

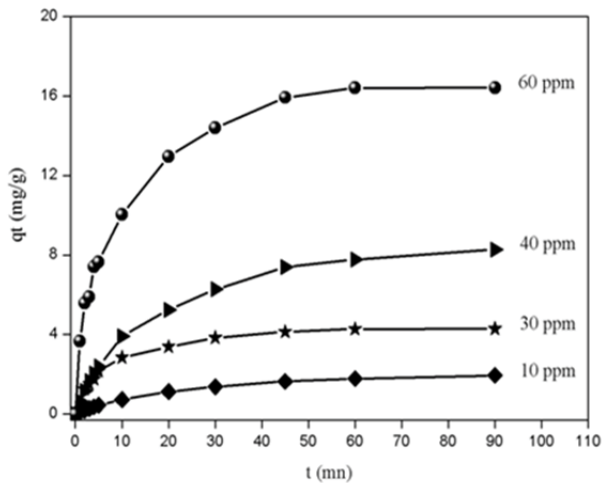

Fig. 6. Effect of contact time and dye concentration on removal of IC by AC.

classification of isotherms is given by Giles et al. [19]. In our case, the isotherm of IC on AC displays *L* and *S* shapes. The initial part of the *L* curve indicates a small interaction of IC/adsorption sites at low concentrations, but when the concentration C_0 in the liquid phase increases, the adsorption occurs more readily. Such behavior is due to a synergistic effect with the adsorbed IC, facilitating the uptake of additional ions as a result of attractive interactions of adsorbate-adsorbate.

Five models have been tested for the adsorption equilibrium: Langmuir (Fig. 7(a)), Freundlich, Temkin, Elovich, and Dubinin-Radushkevich (Fig. 7(b)) are used in the present study, and their applicability is compared.

3.3.1. Langmuir isotherm

The Langmuir isotherm model [20] is based on the assumption that maximum adsorption corresponds to a saturated monolayer of solute molecules on the adsorbent surface. The linear form of the isotherm equation is given by

$$\frac{1}{C_e} = K_L\, q_{\max} \times \frac{1}{q_e} - K_L \tag{5}$$

where C_e is the equilibrium concentration (mg/L), $q_{\max}$ the monolayer adsorption capacity (mg/g), and K_L the constant related to the free adsorption energy (L/mg).

3.3.2. Freundlich isotherm

The linear form of the isotherm model is represented by the following equation [21]:

$$\ln q_e = \ln K_F + \frac{1}{n} \ln C_e \tag{6}$$

K_F is a constant indicative of the adsorption capacity (L/g) and *n* an empirical constant related to the adsorption driving force.

3.3.3. Temkin isotherm

The Temkin linearized model is given by [22]

$$q_e = \frac{RT}{b} \times \ln AC_e = B \ln A + B \ln C$$

C_e is the equilibrium concentration (mg/L), [illegible] and *b* are the Temkin constants, *R* is the universal gas constant, and *q* (mg/g) the adsorption capacity. The theoretical parameters of adsorption isotherms along with correlation coefficients, RMSE, SSE, and χ^2 are presented in Table 1. The small the RMSE and χ^2 values better the curve fitting.

The nature of adsorption is expressed in terms of dimensionless separation factor of equilibrium parameter:

$$R_L = \frac{1}{1 + K_L C_e} \tag{8}$$

The R_L value indicates the type of isotherm: (R_L = 0) reversible, (0 < R_L < 1) favorable, (R_L = 1) linear, and (R_L > 1) unfavorable.

In this study, R_L lies between 0.74 and 0.90 over the C_0 range (20–60 mg/L). R_L is less than 1, confirming that the IC

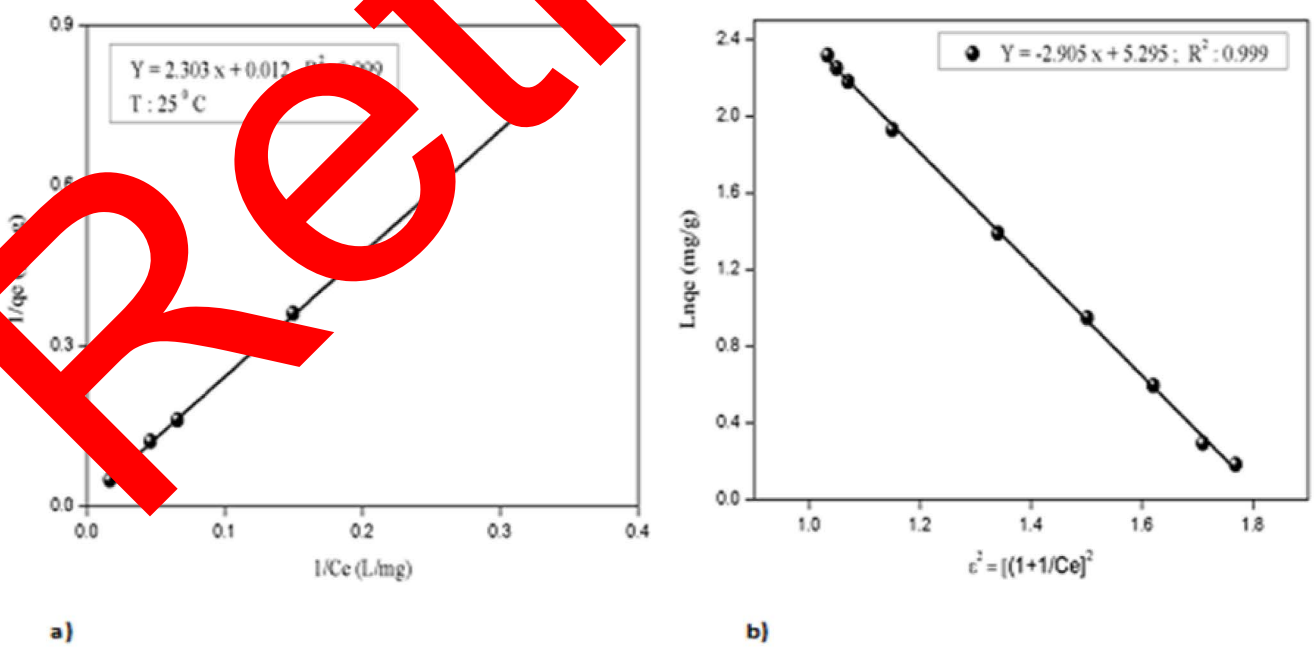

Fig. 7. (a) Langmuir isotherm model for the adsorption of IC onto AC and (b) Dubinin-Radushkevich isotherm model for the adsorption of IC onto AC.

Table 4
Sorption isotherm coefficients of different models

	Langmuir	Freundlich	Temkin	Dubinin-Radushkevich	Elovich
40°C		$1/n$: 0.703	B: 3.14	K: 11.2 × 10^{-4} mol² k/J²	
K_L	0.0058 L/mg				K_E: [illegible] 10^{-5} L/mg
q_{max}	79.49 mg/g	K_F: 0.759 mg/g	A_T: 0.51 L/mg	q_{max}: 298.34 mg/g	q_{max}: 11[illegible] g/g
			ΔQ: 65.52 kJ/mol	E: 21.18 kJ/mol	
RMSE	35.188	44.236	65.236	1.1885	[illegible].123
R^2	0.944	0.896	0.897	0.996	[illegible]37
25° C		$1/n$: 0.926	B: 6.24	K: 0.0014 mol² k/J²	
K_L	5.2 × 10^{-3} L/mg	K_F: 0.477 mg/g	A_T: 0.265 L/mg	q_{max}: 459 mg/g	
q_{max}	83.33 mg/g		ΔQ: 0.39 kJ/mol	E: 19.047 J/mo[illegible]	
RMSE	7.255	45.410	41.69	[illegible]338	
R^2	0.999	0.926	0.864	0.[illegible]	

adsorption on AC is favored in both cases with the successful applicability of Langmuir isotherm.

3.3.4. Dubinin-Radushkevich isotherm

The Dubinin-Radushkevich isotherm can be used to describe the adsorption on both homogenous and heterogeneous surfaces [23]:

$$\ln q_e = \ln q_m - \beta\varepsilon^2 \tag{9}$$

where q_m is the Dubinin-Radushkevich mono[illegible] capacity (mg/g), β a constant related to sorption [illegible]ergy, and the Polanyi potential which is related to [illegible] equilibrium concentration as follows:

$$\varepsilon = RT\ln\left(1+\frac{1}{C_e}\right) \tag{10}$$

where R is the gas co[illegible]nt (8.[illegible]/mol K) [illegible] is the absolute temperature. [illegible]e const[illegible] β gives the mean free energy E of adsorptio[illegible]er m[illegible]ule o[illegible]e adsorbate when it is t[illegible]d to the [illegible]rf[illegible] of the s[illegible]d from infinity in the [illegible]ation [illegible] can be [illegible]uted usin[illegible]e relation:

$$E = \frac{1}{\sqrt{2\beta}} \tag{11}$$

Th[illegible]agnitude of E is useful for estimating the ad[illegible]ion mechanism.

I[illegible] case of E < 8 kJ/mol, physical forces may affect the adsorpt[illegible] Conversely, if E is in the range of 8–16 kJ/mol, adsorption [illegible]verned by ion exchange mechanism.

3.3.5. Elovich isotherm

The Elovich isotherm [24] is based on the principle of the kinetic assuming that the number of adsorption sites increases exponentially with the adsorption, which implies a multilayer adsorption:

$$\ln\frac{q_e}{C_e} = \ln q_m \times K_E - \frac{q_e}{q_m} \tag{12}$$

where K_E (L/mg) is the [illegible]vich constant at equilibrium, q_{max} (mg/g) [illegible]imum a[illegible]pti[illegible] capacity, q_e (mg/g) the adsor[illegible]n capacity at equ[illegible]m, and C_e (g/L) the equilibriu[illegible] concentratio[illegible]f the adsorbate. The equilibrium const[illegible] and the max[illegible]m capacity can be calculated from the pl[illegible] $\ln(q_e/C_e)$ vs.[illegible]

3.[illegible] Adsorption kinetics

T[illegible]etic study is important for the adsorption process becaus[illegible] only it describes the uptake rate of adsorbate but also c[illegible]trols the residual time of the whole process, and two mod[illegible] are selected to describe the adsorption process.

[illegible]he pseudo-first-order equation is given by [25]

$$\log\left(q_e - q_t\right) = \log q_e - \frac{k_1}{2.303}\times t \tag{13}$$

While the pseudo-second-order model [26] is given by

$$\frac{t}{q_t} = \frac{1}{k_2 q_e^2} + \frac{1}{q_e}\times t \tag{14}$$

where q_t (mg/g) is the amount of IC adsorbed on AC at the time t (min) and K_1 (min^{-1}) and K_2 (g/mg min) are the pseudo-first-order and pseudo-second-order kinetic constants, respectively.

The Elovich equation is a kinetic equation related to the chemisorption process and is validated for systems where the surface of the adsorbent is heterogeneous; the linear form is given as follows:

$$q_t = \left(\frac{1}{\beta}\right)\ln\alpha\beta + \left(\frac{1}{\beta}\right)\ln t \tag{15}$$

where α (mg/g min) is the initial adsorption rate and β (mg/g) the relationship between the degree of surface coverage and the activation energy involved in the chemisorption. The rate constants predict the uptakes and the corresponding correlation coefficients for AC summarized in Table 5. For the pseudo-first-order kinetic (Fig. 8(a)), the experimental data

Table 5
Kinetic and intraparticle parameters for the IC adsorption onto AC

C_0 (mg/L)	Pseudo-second order					Pseudo-first order			
	q_{ex} (mg/g)	q_{cal} (mg/g)	R^2	$\Delta q/q$ (%)	K_2 (g/mg min)	q_{cal} (mg/g)	R^2	$\Delta q/q$ [illegible]	K_1 (min^{-1})
10	2.40	2.448	0.999	1.96	0.018	1.884	0.999	5.52	[illegible]0403
30	4.50	4.589	0.998	1.94	0.0383	4.092	0.956	6.16	[illegible]
40	9.50	9.681	0.999	1.87	0.0069	7.586	0.996	2.56	[illegible]
60	17.35	17.575	0.999	1.28	0.0100	16.226	0.929	1.07	0.0945

C_0 (mg/L)	Elovich			C_0 (mg/L)	Diffusion			
	R^2	β (g/mg)	α (mg/g min)		K_{in} (mg/g min$^{1/2}$)	R^2	C (mi[illegible]	D cm^2/s
10	0.964	2.123	–1.931	10	0.09	[illegible]	[illegible]	
30	0.983	27.174	2.023	30	0.32	0.964	[illegible]	4.5×10^{-7}
40	0.985	0.529	–13.731	40	0.36	0.996	[illegible].571	
60	0.986	0.316	2.710	60	[illegible]	[illegible]	5.53	

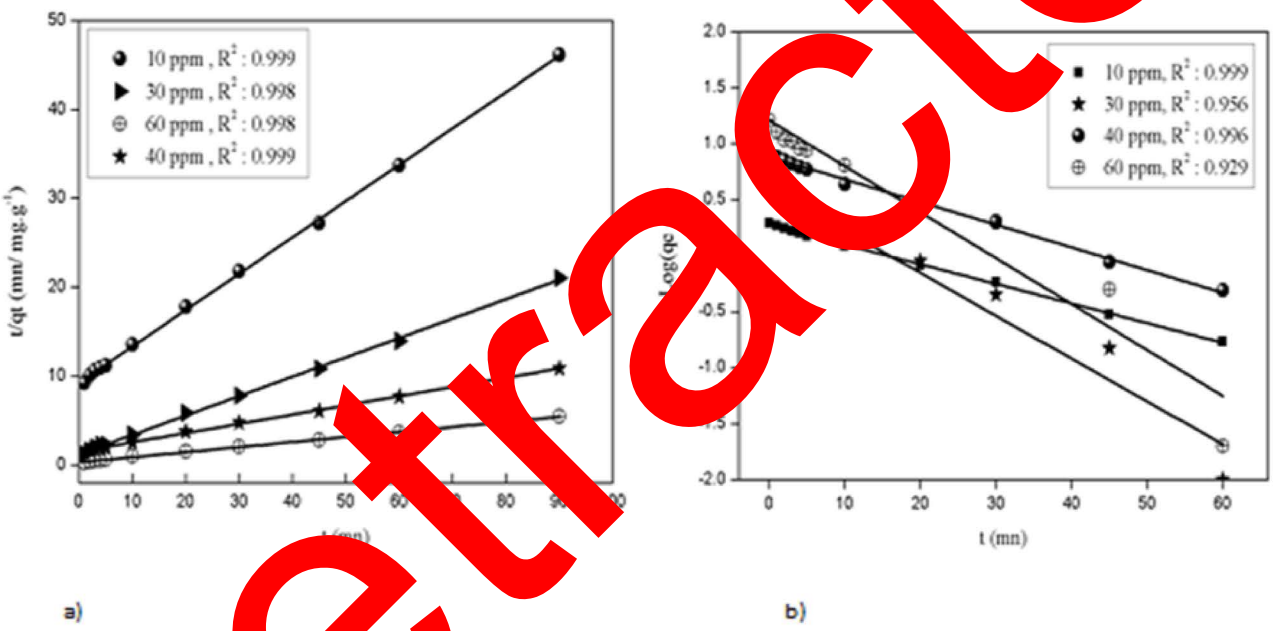

Fig. 8 [illegible]do-secon[illegible]d [illegible]inetic pl[illegible] for the adsorption of IC onto AC and (b) First-order kinetic plot for the adsorption of IC [illegible]o AC

deviate from [illegible]earity as evidenced from the low values of [illegible] and C_0 [illegible] applicable for the present sys[illegible] By [illegible]ntrast, the cor[illegible]tion coefficient and $q_{e,cal}$ determ[illegible]om the pseudo-second-order kinetic model agree with [illegible]xperimental data (Fig. 8(b)). Its applicability suggests tha[illegible] adsorption of IC onto AC is based on chemical reaction (c[illegible]sorption), involving an exchange of electrons between ads[illegible]ent and adsorbate. In the chemisorptions, the IC ions are attached to the adsorbent surface by chemical bond and tend to find sites that maximize their coordination number with the surface.

3.5. Intraparticle diffusion study

The mechanisms and kinetics of the adsorption are described by various models, which predict the breakthrough curves at different times and accuracies. Nevertheless, there are not clear criteria to decide which model is convenient for a given case:

- The involved mass transfer resistances,
- Relation type between the adsorbed amount and the diffusion coefficients,
- Definitive equilibrium equation,
- Description level and the mathematical complexity of the model,

It is well known that a performed batch experiment gives valuable data to evaluate the diffusion coefficients. Under real conditions, the mass transport resistance in the solid is larger than the external fluid film on the solid particles. The possibility of intraparticle diffusion [27] during the transportation of adsorbate from solution to the particle

surface was also investigated by the intraparticle diffusion model:

$$q_t = K_{in}\sqrt{t} + C \tag{16}$$

where K_{id} is the intraparticle diffusion rate constant (mg/g min$^{1/2}$), q_t the amount of IC adsorbed at time t, and C (mg/g) the intercept. The plot of q_t versus $t^{1/2}$ enables to determine both K_{id} and C (Fig. 9). The mechanism of adsorption is complex, but the intraparticle diffusion is important in the early stages.

The first linear part could be due to intraparticle diffusion effects whose slopes are defined as the rate parameters, characteristic of the adsorption rate in the region where the intraparticle diffusion occurs.

Initially and within a short period, it is postulated that IC ions are transported to the AC external surface through the film diffusion with a high rate.

Once the surface is saturated, the IC ions enter inside AC by intraparticle diffusion through the pores and internal surface diffusion until equilibrium is reached, and this is represented by the second straight lines.

The data collected at 25°C for an initial IC concentration (20–60 mg/L) exhibit multilinear plots (Table 5). These results indicate that two or more steps occur during the adsorption process. Therefore, some boundary layer control must be involved, and the intraparticle diffusion is not the limiting step.

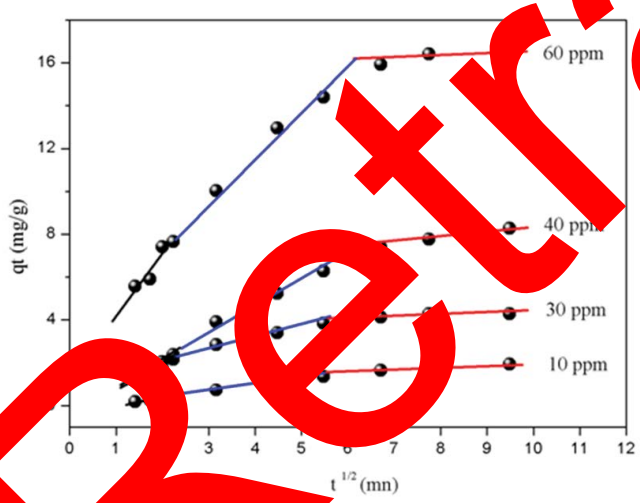

Fig. 9. Application of intraparticle diffusion for the adsorption of IC onto AC.

3.6. Effect of temperature

The adsorption reaction of coloring molecules on a surface implies a variation of the free energy $\Delta G°$ (kJ/mol) (variation of energy at constant pressure) between the initial and final states which predicts the feasibility of a reaction.

$$\Delta G° = \Delta H° - T\Delta S° \tag{17}$$

The energy of Gibbs is composed of two terms: an enthalpy term H which expresses the energies of interactions between the molecules and the adsorbent surface and an entropic term S which expresses the ramification and arrangement of the molecules in liquid phase and on the surface. The thermodynamic behavior of adsorption of IC on AC was further investigated. The thermodynamic parameters ($\Delta G°$), enthalpy ($\Delta H°$) and entropy ($\Delta S°$) are calculated using the following equation:

$$\Delta G° = -RT\ln K_e \tag{18}$$

where K_e is the apparent equilibrium constant. The apparent enthalpy ($\Delta H°$) of the adsorption and entropy ($\Delta S°$) of the adsorption are calculated from adsorption data at different temperatures using Eq. (19). The adsorption capacity of AC increases with raising temperature over the range 303–313 K, and beyond this range, the vaporization becomes an increasing problem. The insights of the adsorption mechanism can be determined from the free energy ($\Delta G°$), enthalpy ($\Delta H°$), and entropy ($\Delta S°$). In the rate law, the temperature dependence appears in the rate constant, and over a limited range, it can usually be represented by Eqs. (19) and (20). The thermodynamic equilibrium constant (K) was determined by Khan and Singh [28] by plotting $\ln(q_e/C_e)$ vs. q_e and extrapolating to zero q_e. The thermodynamic parameters are determined from the following equations:

$$\ln K_e = \frac{\Delta H°}{R} \times \frac{1}{T} - \frac{\Delta S°}{R} \tag{19}$$

The plot of $\ln K_e$ $1/T$ is linear, and $\Delta H°$ and $\Delta S°$ are obtained from the slope and intercept of the Van't Hoff Eq. (16), while $\Delta G°$ at various temperatures is reported in Table 6. The positive $\Delta G°$ indicates a not spontaneous process, while the positive $\Delta H°$ and $\Delta S°$ show that the IC adsorption on AC is endothermic with an increased randomness at the solid-solution interface.

The rate constant and the dependence of rate constants on temperature over a limited range can usually be represented

Table 6
Thermodynamic parameters for the IC adsorption onto AC

T (K)	K_e	R^2	$\Delta G°$ (kJ/mol)	$\Delta H°$ (kJ/mol)	$\Delta S°$ (kJ/mol k)	E_a (kJ/mol)
303	1.028	0.999	–0.0705			
307	1.231	0.989	–0.5310	28.115	0.093	51.065
310	1.363	0.997	–0.8512			
317	1.497	0.988	–1.0503			

by Eq. (20). The adsorption capacity of AC increases with raising temperature in the range 299–313 K.

$$\ln K_2 = \ln A - \frac{E_a}{RT} \tag{20}$$

A is the pre-exponential factor, E_a the activation energy, and K_2 (g/mg min) the pseudo-second-order kinetic constant at different temperatures. E_a is obtained by plotting $\ln K_2$ against $1/T$. All the calculated thermodynamic parameters are presented in Table 6.

3.7. Comparative study of the adsorption capacity of IC by the different adsorbents

It is instructive for a comparative purpose to report the values of the adsorption capacity of some adsorbents available in the literature (Table 7). One can see that the IC adsorption observed in this work is well positioned with respect to other researches. For our study, the maximum adsorption capacity was found to be 79.49 mg/g at 25°C and 298.34 mg/g at 40°C at pH 2. The differences of dye uptake are due to the properties of each adsorbent like the structure, the functional groups, and the surface area. AC could be an attractive adsorbent for basic dyes owing to the isoelectric point (pH_{pzc}).

Table 7
Adsorption capacities of IC by various adsorbents

Adsorbant	q_{max} (mg/g)	References
Activated carbon	298.34	This stu
Activated carbon-based KOH	13.40	[29]
Silk	18.38	[33]
Calcined (Zn/Al + Fe) layered double hydroxide	488.93	[1]
TiO_2/UV/O_2	14.28	[32]
Mesoporous Mg/Fe layered doub hydroxide nanoparticles	62	[3]
Nanofiber membranes	2	[34]
Acacia nilotica (Babool) sawdust activated carbon	37.91	[35]
Chitosan	2.82	[5]
Carbonaceous material om pyrolv vage slud	92.8	[37]
Br l	31	[7]
oporous p acrylic ac 11 composite na ber membranes		[38]
Maize cob	118.48	[39]
itin n hisker zed n PFM	72.66	[40]
Ap tone activated carbon	552.55	[41]
Rice hu h	29.28	[2]
Mesoporo lyvinyl alcohol/SiO_2 nanofiber me branes	495.00	[42]
Urea-treated cellulosic waste of citrus reticulata peels	71.07	[43]
Ni nanoscale oxides/*Schoenoplectus acutus* composite	860.23	[44]
Activated sewage sludge	60.04	[45]
Nanocomposite hydrogels	370.37	[46]

4. Conclusions

The adsorption characteristics of IC onto gly affected by the initial dye concentration itial pH, adsorbent dose. A pH value of 2 was orable for t optimum adsorption of IC dye by AC. T R_L values an other adsorption parameters indicating e Dubinin Radushkevich and Langmuir mo rovi a better fit of the equilibri adsorp data ey gave a maximum adsorptio apacity 79.49 mg/g at 25°C which increas d up to 298 mg/ t 40° t pH 2. This study has sho tha the A e emplo d as effective adsorbent for th oval of om aque solution. The pseudo-second- odel ga escription of the kinetic data.

The n free e y $\Delta G°$ and positive enthalpy $\Delta H°$ in ated that the ads of IC onto AC is spontaneo and endother ic over the studied temperature range e positive en py $\Delta S°$ clearly states that the randomne increased at e solid-solution interface during e IC a tion on C, indicating that some structural ange among the active sites of the adsorb d the ions. The adsorption of IC ions by AC follows se second-order kinetic model, which relies on the ssump at the chemisorptions may be the rate-limiting step; t IC ions are attached to the adsorbent surface by formi a chemical bond and tend to find sites that maxi- eir coordination number with the surface. This study in tiny batch gave rise to encouraging result, and we wish to achieve the adsorption tests in column mode under the conditions applicable to the treatment of industrial effluents, and the present investigation showed that AC is a potentially useful adsorbent for the dyes.

Future applications of the current work:

- Contribute to the reduction of environmental pollution, which remains a major international problem.
- Create agreements between the laboratory and the textile industry.
- Switch from batch mode to column mode.
- Realization of tests on an industrial scale.
- Perform theoretical simulations of phenomena.
- Preparation of new adsorbents at low economic cost.
- Elimination of pollutants by solar photodegradation.

Using the homogeneous photodegradation of IC on SnO_2 semiconductor is the future objective of this work. Preliminary tests were satisfactory; the experiments are currently under way and will be reported very soon.

Acknowledgements

The authors gratefully acknowledge support from University M'hamed Bougara of Boumerdes, Laboratory of Soft Technologies and Biodiversity, Faculty of Sciences, Chemistry Department.

References

[1] T.I. Tikhomirova, G.R. Ramazanova, V.V. Apyari, Effect of nature and structure of synthetic anionic food dyes on their sorption onto different sorbent peculiarities and prospect, Microchem. J., 143 (2018) 305–331.

[2] U.R. Lakshmi, V.C. Srivastava, I.D. Mall, D.H. Lataye, Rice husk ash as an effective adsorbent: evaluation of adsorptive characteristics for Indigo Carmine dye, J. Environ. Manage., 90 (2009) 710–720.

[3] T. Nakamura, N. Kawasaki, S. Tanada, T. Tamura, Y. Shimizu, Indigo carmine removal by charcoal from rice bran as an agricultural by-product, Toxicol. Environ. Chem., 87 (2005) 321–327.

[4] Y. Lu, J. Li, X. Zhang, J. Tang, B. Wei, J. Liu, Studies on the mechanism of Indigo Carmine removal by solvent sublation, J. Colloid Interface Sci., 292 (2005) 210–218.

[5] L.P. Donald, M.L. Gray, S.K. George, Introduction to Organic Laboratory Techniques: A Contemporary Approach, W.B. Saunders, U.S.A., 1976.

[6] K. Lacasse, W. Baumann, Textile Chemicals: Environmental Data and Facts, Springer, New York, 2004.

[7] A.G.S. Prado, B.S. Miranda, G.V.M. Jacintho, Interaction of indigo carmine dye with silica modified with humic acids at solid/liquid interface, Surf. Sci., 542 (2003) 276–282.

[8] M. Nourozi, T. Chuah, S. Thomas, Adsorption of reactive dyes by palm kernel shell activated carbon: application of film surface and film pore models, E-J. Chem., 6 (2009) 949–954.

[9] R. Malarvizhi, N. Sulochana, Sorption isotherm and kinetic studies of Methylene blue uptake onto activated carbon prepared from wood apple shell, J. Environ. Prot. Sci., 2 (2014) 40–60.

[10] C. Min-Shen, H. Pang-Yen, L. Hasing-Ya, Adsorption behav[illegible] of dye AAVN and RB4 in acid solutions on chemically [illegible]s-linked chitosan beads, J. Chin. Inst. Chem. Eng., 34 [illegible]003) 625–634.

[11] J.N. Nsami, J.K.M. Mbadcam, The adsorption effici[illegible] of chemically prepared activated carbon from co[illegible]t shells by $ZnCl_2$ on methylene blue, J. Chem., 201 (2013) [illegible].

[12] B. Sumalatha, Y. Kumar, K. Kiran, J. Babu, N[illegible]ata, D. Maria[illegible] T. Venkateswarulu, Removal o[illegible]ndigo carm[illegible]om aqueous solution by using activated ca[illegible] B[illegible]J. Pha[illegible]Biol. Chem. Sci., 5 (2014) 912.

[13] Z. Harrache, M. Abbas, T. Aks[illegible]rari, Therm[illegible]amic and kinetics studies on adsorption o[illegible]ligo Carm[illegible]om aqueous solution by activated carbon, [illegible]rochem. J., 144 (2019) 180–189.

[14] M. Abbas, T. Aksil, M[illegible]rari, R[illegible]al of tox[illegible]yl green (MG) in aqueous so[illegible]ions by [illegible]cot stone activated carbon - equilibrium and i[illegible]herms [illegible]eling [illegible]esal. Wat. Treat., 125 (2018) 93–101.

[15] [illegible] J.K. Mb[illegible] D.T. Tchui[illegible], J.N. Nsami, Kinetic [illegible]d equi[illegible]m stud[illegible] the adsor[illegible]n of Mercury (II) ions from aque[illegible] solution t[illegible] and metakaolinite clays from sout[illegible]n Cameroon, I[illegible]es. Chem. Environ., 3, N++ 2013 (201[illegible]–11.

[16] M. Abb[illegible] M. Trari, Kinetic and equilibrium studies of c[illegible] adsorp[illegible]cot stone activated carbon, J. Ind. E[illegible]hem., 20 (2014) 745–751.

[17] [illegible] Abbas, M. Trari, Kinetic, equilibrium and thermodynamic [illegible] on the removal of Congo red from aqueous solutions by ad[illegible]ion onto apricot stone, Process Saf. Environ. Prot., 98 (2015) [illegible]436.

[18] M. Abb[illegible] Abdelhamid, K. Samia, A. Tounsia, Adsorption in simple batch experiments of Coomassie blue G-250 by apricot stone activated carbon—Kinetics and isotherms modeling, Desal. Wat. Treat., 57 (2016) 15037–15048.

[19] GH. Giles, T.H. MacEwan, S.N. Nakhwa, D. Smith, Areas of solids, J. Chem. Soc., 10 (1960) 3973–3993.

[20] I. Langmuir, The adsorption of gases on plane surfaces of glass, mica and platinum, J. Am. Chem. Soc., 40 (1918) 1361–1403.

[21] H.M.F. Freundlich, Über die Adsorption in Lösungen, Z. Phys. Chem. (Leipzig), 57A (1906) 385–470.

[22] M.I. Temkin, V. Pyzhev, Recent modifications to Langmuir isotherms, Acta Phys., 12 (1940) 327–356.

[23] T. Shahwan, H.N. Erten, Temperature effects in barium sorption on natural kaolinite and chlorite-illite clays, J. Radioanal. Nucl. Chem., 260 (2004) 43–48.

[24] M. Ghaedj, F. Karimi, B. Barrazzch, R. Sab[illegible]i, A. Danichfar, Removal of Reactive Orange 12 from aqu[illegible] solutions by adsorption on tin sulfide nanoparticle loade[illegible] activated carbon, J. Ind. Eng. Chem., 19 (2013) 756.

[25] S. Lagergren, About the theory of so-call[illegible]on of soluble substances, Kung. Vetensk.akad. H[illegible], 24 (19[illegible]39.

[26] Y.S. Ho, G. McKay, Kinetic models for the [illegible]ption of dye [illegible] aqueous solution by wood, J. Environ. Sc[illegible]ealth. B, 76 (19[illegible] 183–191.

[27] T.W. Weber, R.K. Chackravorti, Kinetics of a[illegible]tion on carb[illegible] from solution, J. Sanit. Eng. Div[illegible]963) 31[illegible]

[28] A.A. Khan, R.P. Singh, [illegible]sorp[illegible]therm[illegible] of carbofuran on Sn (IV) ars[illegible]silicate in[illegible] Na^+ and $Ca^{[illegible]}$ forms, Colloids Surf., 24 (1987) 3[illegible]42.

[29] A.N. Od[illegible]ru, K. Da[illegible]a, B[illegible]. Des[illegible] N.J. Nsami, K.J. Mbad[illegible] Re[illegible]oval [illegible]nd[illegible] carmine [illegible]e (IC) by batch adsorption [illegible] onto [illegible]cola nut s[illegible]s and its active carbon from [illegible]us medi[illegible]Int. J. [illegible] Res. Technol., 5 (2016) 874–8[illegible].

[30] N. Jiwalak, S. Rat[illegible]hani, J.B. Bremner, V. Rattanaphani, Equil[illegible]d kine[illegible]odeling of the adsorption of indigo ca[illegible]ne onto silk, Fibers [illegible] (2010) 572–579.

[31] H[illegible]éssaha, M. Bouraada, L[illegible]éménorval, Removal of indigo c[illegible]ine and gree[illegible]ezanyl-F2B from water using calcined a[illegible]uncalcined Zn/[illegible] Fe layered double hydroxide, J. Water D[illegible] 7 (2017) 152–[illegible].

[32] S. [illegible]ane, S. [illegible]rzal, M. El Ouardi, M. Belmouden, A. As[illegible]Ait-Ichou, Adsorption and photocatalytic [illegible]egradation of indigo carmine dye in aqueous solutions using [illegible]/UV/O_2, J. Mater. Environ. Sci., 4 (2013) 239–250.

[33] M[illegible]Ahmed, A.A. Brick, A.A. Mohamed, An efficient ad[illegible]n of indigo carmine dye from aqueous solution on m[illegible]pporous Mg/Fe layered double hydroxide nanoparticles [illegible]pared by controlled sol-gel route, Chemosphere, 174 (2017) [illegible]0–288.

[illegible] M. Li, H. Wang, S. Wu, F. Li, P. Zhi, Adsorption of hazardous dyes indigo carmine and acid red on nanofiber membranes, RSC Adv., I3, (2012) 900–907.

[35] T.B. Gupta, D.H. Lataye, Adsorption of indigo carmine dye onto *Acacia nilotica* (babool) sawdust activated carbon, J. Hazard. Toxic Radioact. Waste, 21 (2017).

[36] A.G.S. Prado, J.D. Torres, E.A. Faria, S.C.L. Dias, Comparative adsorption studies of indigo carmine dye on chitin and chitosan, J. Colloid Interface Sci., 277 (2004) 43–47.

[37] E. Gutiérrez-Segura, M. Solache-Ríos, A. Colín-Cruz, Sorption of indigo carmine by a Fe-zeolitic tuff and carbonaceous material from pyrolyzed sewage sludge, J. Hazard. Mater., 170 (2009) 1227–1235.

[38] R. Xu, M. Jia, F. Li, H. Wang, B. Zhang, J. Qiao, Preparation of mesoporous poly (acrylic acid)/SiO_2 composite nanofiber membranes having adsorption capacity for indigo carmine dye, Appl. Phys. A, 106 (2012) 747–755.

[39] J. Zhang, P. Zhang, S. Zhang, Q. Zhou, Comparative study on the adsorption of tartrazine and indigo carmine onto maize cob carbon, J. Sep. Sci. Technol., 49 (2014) 877–886.

[40] S. Gopi, P. Balakrishnan, A. Pius, S. Thomas, Chitin nanowhisker (*ChNW*)-functionalized electrospun PVDF membrane for enhanced removal of Indigo carmine, Carbohydr. Polym., 165 (2017) 115–122.

[41] H.M.H. Gad, A. El-Hakim, A.M. Daifullah, Impact of surface chemistry on the removal of indigo carmine dye using apricot stone active carbon, Adsorpt. Sci. Technol., 25 (2007) 327–341.

[42] M. Teng, F. Li, B. Zhang, A.A. Taha, Electrospun cyclodextrin-functionalized mesoporous polyvinyl alcohol/SiO_2 nanofiber membranes as a highly efficient adsorbent for indigo carmine dye, Colloids Surf. A Physicochem. Eng. Asp., 385 (2011) 229–234.

[43] R. Rehman, J. Zafar, H. Nisar, Adsorption studies of removal of indigo caramine dye from water by formaldehyde and urea treated cellulosic waste of citrus reticulate peels, Asian J. Chem.; 26 (2014) 43–47.
[44] S. Sánchez-Rodríguez, J. Trujillo-Reyes, E. Gutiérrez-Segura, M. Solache-Ríos, A. Colín-Cruz, Removal of indigo carmine by a Ni Nanoscale oxides/*schoenoplectus acutus* composite in batch and fixed bed column systems, Sep. Sci. Technol., 50 (2015) 1602–1610.
[45] M. Otero, F. Rozada, L.F. Calvo, A.I. García, A. Morán, Elimination of organic water pollutants using adsorbents obtained from sewage sludge, Dyes Pigm., 57 (2003) 55–65.
[46] M. Dalaran, S. Emik, G. Güçlü, T.B. İyim, S. Özgümüş, Study on a novel polyampholyte nanocomposite superabsorbent hydrogels: Synthesis, characterization and investigation of removal of indigo carmine from aqueous solution, Desalination, 279 (2011) 170–182.